International Journal of Nanoelectronics and Materials
Volume 14 (Special Issue) December 2021 [149-155]

UniMAP UNIVERSITI MALAYSIA PERLIS

Analysis of Stability of Nano- vs Micro-sized Resonant Tunnelling Diode (RTD) Devices for Future Neuromorphic Computing Applications

Qusay Raghib Ali Al-Taai[1*], Jue Wang[1], Razvan Morariu[1], Afesomeh Ofiare[1], Abdullah Al-Khalidi[1] and Edward Wasige[1]

[1] High-Frequency Electronics group, division of Electronics and Nanoscale Engineering, James Watt School of Engineering, University of Glasgow, Glasgow, G12 8LT, United Kingdom.

ABSTRACT

In this paper, we report on the fabrication of micrometre and nanometre-sized resonant tunnelling diode (RTD) devices which may be used as excitable neuromorphic spike generators. The fabrication processes using photolithography were applied for micro-sized RTDs, while for nano-RTDs the fabrication was optimised to achieve accurate nano-sized mesas through a multi-exposure step based on e-beam lithography. The results show a large decrease in the peak currents from 41 mA to 27 μA for micro- and nano-RTDs, respectively, peak and valley voltages of around 0.6 V and 0.8 V and a peak to valley current ratio of around 2.4. For the smallest fabricated RTD of 300 nm diameter, the expected energy consumption per oscillation cycle (if used in an oscillator) will be 1.55 fJ. DC characterisation of the devices show that the nano-RTDs are stable and have smooth current voltage (I-V) characteristics compared with micro-RTDs. The nano-RTD technology could be employed to realise highly sensitive photodetectors that can be operated as spike generators and so they could underpin the development of energy efficient neuromorphic computing.

Keywords: InP/GaAs, nano electronic devices, nano fabrication, neuromorphic, resonant tunnelling diode.

1. INTRODUCTION

The resonant tunnelling diode (RTD) is a one-dimensional vertical transport unipolar nanoelectronic structure, which is characterised by a highly non-linear *I-V* characteristic comprising a negative differential resistance (NDR) region, and can be used in the design of very high frequency sources and highly sensitive (photo-) detectors, and so are a promising device technology for future terahertz applications [1].

The nanometre-sized RTD (nano-RTD) represents a kind of very low power consumption device, which due to its unique NDR region, can be used in the design of excitable spike (pulsed) generators to produce excitable short electrical and optical pulses mimicking the spiking behaviour of biological neurons thus making it one of the target candidates for such neuromorphic applications [2]. The recent developing of Artificial Intelligence (AI) systems powered by computers that can learn without the need for explicit instructions is transforming our digital economy and our society as a whole. Computational deep neural network models are inspired by information processing in the human brain. However, today's computing hardware, based on von Neumann architectures, is inefficient at implementing these neural networks largely because of the high power consumption per unit area required, typically >10 W/cm^2 compared to around 0.01 W/cm^2 for the human brain [3]. As such, research for new low energy computing paradigms is underway.

*QusayRaghibAli.Al-taai@glasgow.ac.uk

In this paper, we describe an RTD-based optoelectronic device and circuits for high-sensitive photodetectors (down to the few-photon regime). We reduce the RTD's active area (device mesa) to be under 1 μm^2, so that the current passing through the double barrier quantum well (DBQW) at the heart of the device is limited to the micro-Ampere range. This way, we expect to realise an extremely low-power consumption nanodevice. In this paper, we summarize our work on the successful fabrication RTD devices with nanoscale dimensions. We have developed a fabrication process flow that enabled us to fabricate nanowire/nanopillar RTD devices with areas of 0.07 μm^2 and about ~0.196 μm^2 for devices with a top contact diameter of 300 nm and 500 nm, respectively with a good contact resistance [4]. The work has included device characterization, accurate device modelling process and spike generator circuit simulation. The next sections will provide some details about these.

2. EPITAXIAL STRUCTURE DESIGN

The RTD epitaxial wafer structure used in this work was grown on a semi-insulating indium phosphide (InP) substrate using molecular beam epitaxy (MBE) by IQE Ltd. It comprises a double barrier quantum well (DBQW) structure consisting of a 5.7 nm $In_{0.53}Ga_{0.47}As$ quantum well, 1.7 nm AlAs barriers, with one wafer having 100nm and another 250 nm thick lightly doped InAlGaAs spacer layers. The collector and emitter layers are made of highly Si doped $In_{0.53}Ga_{0.47}As$ layers. The 100 nm thick spacer layers were originally incorporated for light absorption in the 1310-1550 nm wavelength range. Details of the epitaxial layer structure are shown in Table 1. We targeted pillar mesa structures with circular geometries with dimensions ranging from 300 nm to 10 μm width/diameter.

Table 1 Structure Specification of 1000A wafer.

Layer	Type	Doping level	Material	Thickness (Å)	Description
12	N++	2.0e19	InGaAs	1000	Contact
11	N+	2.0e18	InAlAs	1000	Collector
10	N-	2.0e16	InAlGaAs	1000	Spacer
9	I	----	InGaAs	20	----
8	I	----	AlAs	17	Barrier
7	I	----	InGaAs	57	Well
6	I	----	AlAs	17	Barrier
5	I	----	InGaAs	20	----
4	N-	2.0e16	InGaAs	200	Spacer
3	N+	2.0e18	InAlAs	1000	Emitter
2	N++	2.0e19	InGaAs	5000	Contact
1	I	----	In(x)AlAs	1000	----
Substrate			InP		

3. DESIGN AND FABRICATION PROCESS

We designed and fabricated mesa structures with circular geometry with diameters of 300, 500, 700 nm for nano-sized devices, and 1, 3, 5, 7, and 10 µm for micro-sized devices. The fabrication of micro- and nano-RTDs is done using a combination of photolithography and e-beam lithography, with the top mesas have been optimised using a combination of dry and chemical wet etching process. In summary, the fabrication process starts with metal evaporation of Ti/Pd/Au to form the top contact of the RTD. Dry etching InGaAs with $Cl_2/CH_4/H_2$ gases at 60˚C to define the RTD mesa. The bottom contact metal (Ti/Pd/Au) was then evaporated. Low dielectric constant polymer benzocyclobutene (BCB) was used for device passivation using multi-baking steps for planarization purposes, followed by etch back process. Finally, bond-pad metallisation was carried out using Ti/Au. Figure1 shows the process flow and Figure2 shows the SEM images for different stages of the fabricated devices.

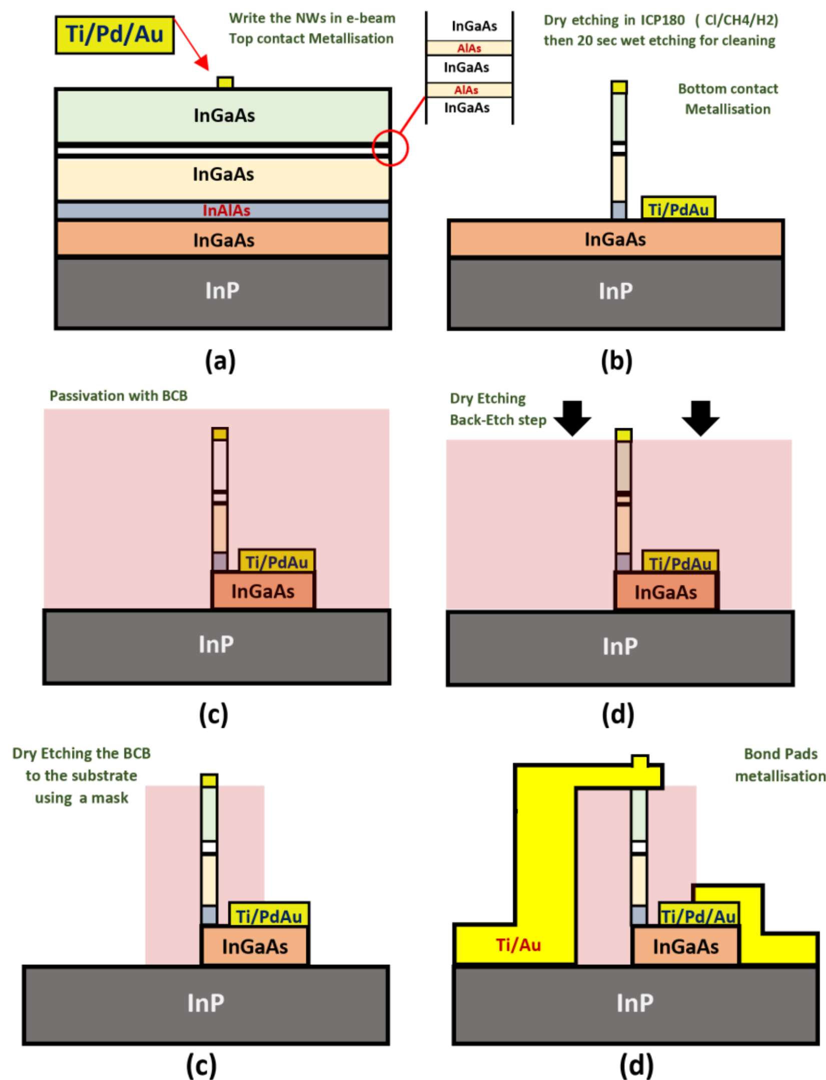

Figure 1. Schematic diagram of the nanofabrication process flow used for the fabrication of micro- and nanopillar RTDs. It consists of the following steps: (a) E-beam lithography patterning of pillars and depositing the top contact; (b) Dry etching by inductively-coupled plasma to bottom contact and depositing the bottom contact; (c) wet etching to substrate, spinning and curing the BCB; (d) blanket dry etch (etch-back) to expose the top metal contact of the RTDs.; (e) dry etch the BCB to open the bottom contact using patterning resist mask; (f) depositing the bond pads.

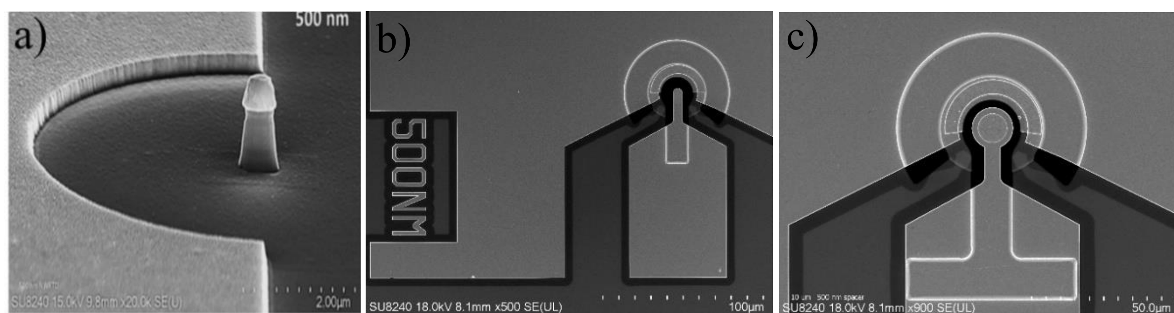

Figure 2. SEM images of a fabricated 500 nm RTD a) top contact/mesa and bottom contact, b) the bond pads of 500 nm completed device, and c) the bond pads of 10 µm completed device.

4. DC CHARACTERISATION

The measured DC current-voltage (*I-V*) characteristics of the fabricated RTDs with diameters from 300 nm to 10 µm are shown in Figure3. The peak DC power consumption is 15.5 µW for 300 nm RTD device which had a peak current of 27 µA at 0.62 V bias voltage, while for the 10 µm diameter RTD it was 41mA at 0.76 V. Therefore, if a 300nm diameter device operated at 10 GHz, the energy consumption per cycle will be 1.55 fJ. The *I-V*s for nano-RTDs are smooth in the NDR region indicating that the devices are stable. The kink or step in the NDR for the larger micro-RTDs is due to bias oscillations.

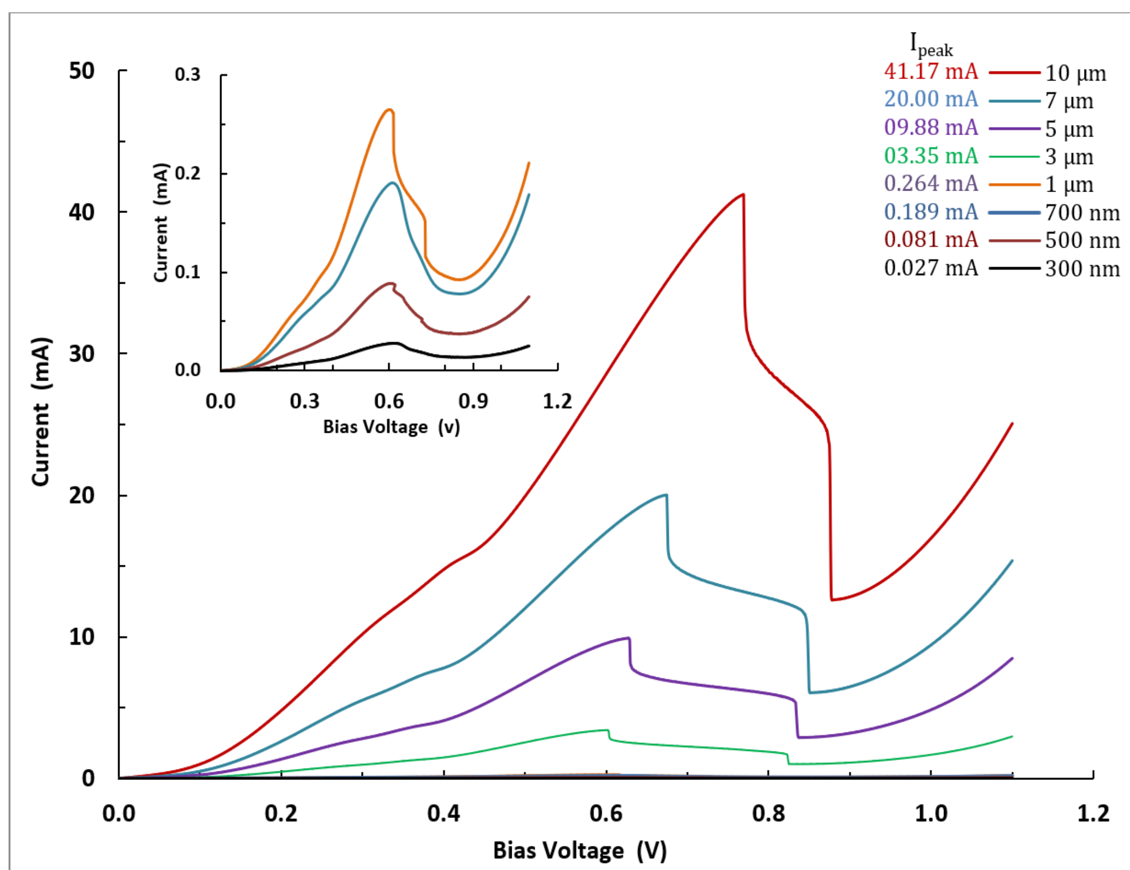

Figure 3. Measured *I-V* characteristics of 300 nm to 10 µm RTD devices. The inset shows a further zoom in over the 300, 500, 700 nm, and 1 µm RTD devices.

5. HIGH FREQUENCY CHARACTERIZATION AND SMALL SIGNAL MODELLING OF MICRO AND NANO RTDS

A vector network analyzer (VNA) was used for high frequency characterisation of the devices. The VNA model is PNA E8361A which goes up to 67 GHz connected to a N5250A millimetre head controller along with a couple of mm Wave test head modules (frequency extenders 67 GHz to 110 GHz model N5262A). The calibration of the VNA was done using the short-open-load-through (SOLT) technique with a port power of −17 dBm. The frequency range was 10 MHz–110 GHz. Figure 4. shows the measured S-parameters (for a bias point in the NDR region) of 300, 500, and 700 nm nano RTDs and 3 µm as an example for a micro-RTD. The nano-RTD devices were stable during measurement and exhibited gain in the reflection coefficient measurement. Micro-RTDs, on the other hand, were unstable in the NDR region and so measurement traces were not smooth, which being clearly exhibiting unexpected jumps (due to interference of bias oscillations in the measurement).

For bias points in the NDR of nano-RTDs, the reflection coefficient S11 (dB) greater than zero for frequencies up to 7.5 GHz, for 300 nm RTD device, 20 GHz for the 500 nm RTD and 30 GHz for the 700nm RTD, indicating that the device provides gain to the input signal (because of the negative differential resistance).

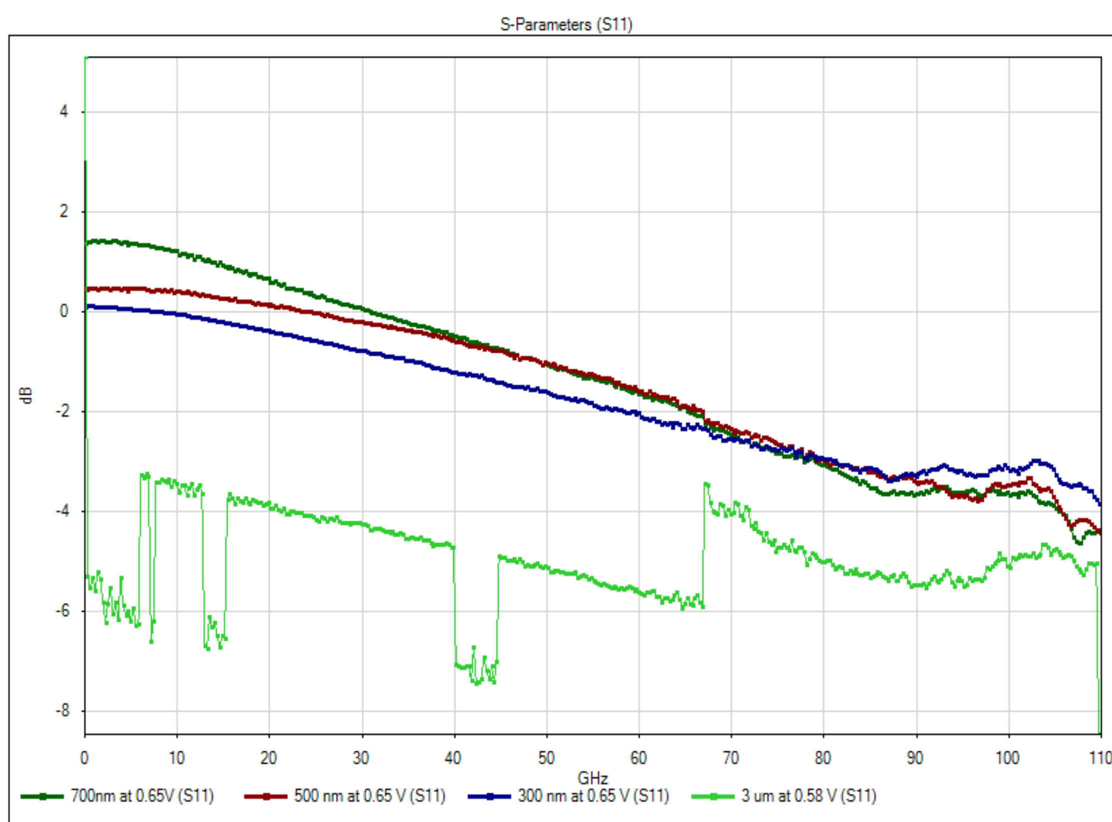

Figure 4. Measured S-parameters (S11) of 300, 500, 700 nm, and 3 µm RTD devices in the NDR region close to the peak voltage.

The small signal equivalent circuit model of the RTD, first introduced in [5] consists of the metal-semiconductor contact and access resistance R_s, in series with the parallel combination of the device self-capacitance C_n together with the device conductance G_n which models the device current–voltage characteristics, and the quantum well inductance L_{qw}, which models the charging and discharging effects of the quantum well [6]. The complete device circuit, shown in Figure 5,

is completed by the extrinsic elements C_p and L_p, which model the parasitic components introduced by the metallic bond-pads [7].

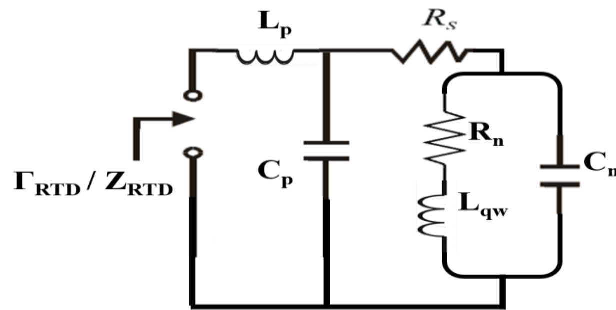

Figure 5. Small-signal equivalent circuit of an RTD device, R_s is the contact and access resistance, which is modelled with the bond-pad parasitic elements (L_p and C_p).

In order to accurately determine the equivalent circuit elements of the fabricated devices, the acquired S-parameter data was first converted to Z-parameters and fitted using the proposed model over the entire frequency range using a direct optimization procedure [8]. Good agreement between measurement and simulation was obtained across the entire bias range and up to 110 GHz for 500 nm nano RTD device compared with 3 μm RTD as illustrated by the graphs in Figure 6 for one bias point (0.65V) in NDR region.

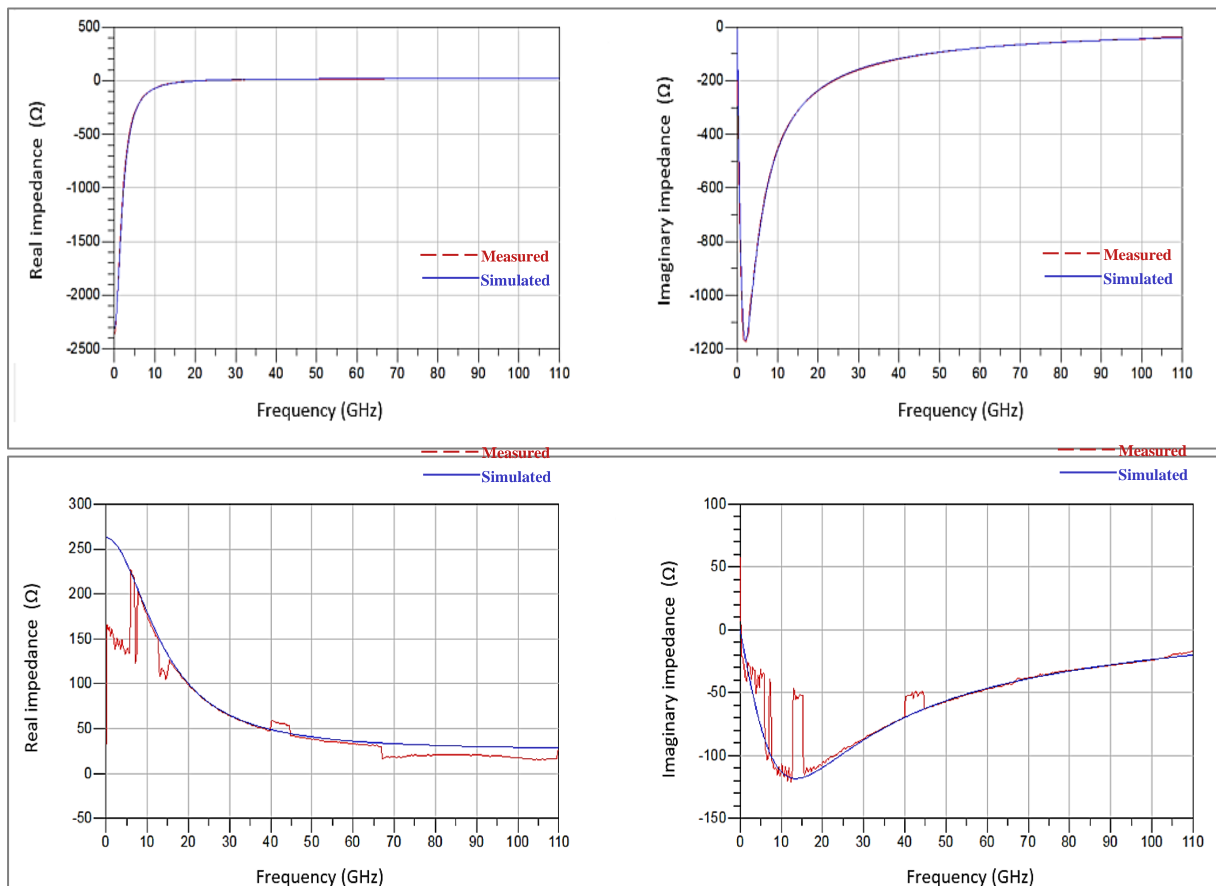

Figure 6. Comparison between measured and modelled equivalent real and imaginary Z-parameters. The dashed lines are for measured, while the sold lines for simulated values, for 500 nm (top), and 3 μm (bottom) diameter device at the NDR region at 0.65V.

6. CONCLUSION

We successfully designed and fabricated nano-RTD devices up to 300 nm diameter. The *I-V* characterization of these devices show extremely low power consumption. The *I-V*s are smooth in the NDR region indicating that the devices are stable. The target application for these devices is in neuron-like spike generators. For bias points in this region, the reflection coefficient S11 (dB) greater than zero for frequencies up to 30 GHz for the 700 nm nano-RTD device, indicating that the device provides gain to the input signal (because of the negative differential resistance). The power consumption in an oscillator circuit can be as low as 1.55 μW per cycle. The RTD includes a light absorption layer and so may be optically controlled.

ACKNOWLEDGEMENTS

The authors would like to thank the staff of James Watt Nanofabrication Centre (JWNC) for assistance in device fabrication. The work was funded by the Horizon 2020 FET-OPEN ChipAI project, grant agreement 828841.

REFERENCES

[1] D. Cimbri, and E. Wasige, "Terahertz Communications with Resonant Tunnelling Diodes: Status and Perspectives in Next Generation Wireless Terahertz Communication Networks", (2021) pp. 25-87.
[2] Romeira, B., Javaloyes, J., Ironside, C. N., Figueiredo, J. M. L., Balle, S., Piro, O., "Excitability and optical pulse generation in semiconductor lasers driven by resonant tunneling diode photo-detectors", Optics Express, Vol **21**, issue 18 (2013) pp. 20931-20940.
[3] Merolla, P. A., Arthur, J. V., Alvarez-Icaza, R., Cassidy, A. S., Sawada, J., Akopyan, F., Jackson, B. L., Imam, N., Guo, C., Nakamura, Y., Brezzo, B., Vo, I., Esser, S. K., Appuswamy, R., Taba, B., Amir, A., Flickner, M. D., Risk, W. P., Manohar, R., Modha, D. S., “A million spiking-neuron integrated circuit with a scalable communication network and interface", Science, Vol **345**, issue 6197 (2014) pp. 668-673.
[4] Marlow, G.S. and Das, M.B., "The effects of contact size and non-zero metal resistance on the determination of specific contact resistance", Solid-State Electronics, Vol **25**, issue 2 (1982) pp. 91-94.
[5] Brown, E.R., Parker, C.D., and Sollner, T.C.L.G., "Effect of quasibound-state lifetime on the oscillation power of resonant tunneling diodes", Applied Physics Letters, Vol **54**, issue 10 (1989) pp. 934-936.
[6] Lake, R., and Y. Junjie, "A physics based model for the RTD quantum capacitance", IEEE Transactions on Electron Devices, Vol **50**, issue 3 (2003) pp. 785-789.
[7] Wang, J., Al-Khalidi, A., Alharbi, K., Ofiare, A., Zhou, H., Wasige E., Figueiredo, J., “High performance resonant tunneling diode oscillators as terahertz sources", 46th European Microwave Conference (EuMC), (2016) pp. 341-344.
[8] Morariu, R., et al., "Accurate Small-Signal Equivalent Circuit Modeling of Resonant Tunneling Diodes to 110 GHz", IEEE Transactions on Microwave Theory and Techniques, Vol **67**, issue 11 (2019) pp. 4332-4340.